

Detailed Expressions and Methodologies for Measuring Flare Combustion Efficiency, Species Emission Rates, and Associated Uncertainties

Darcy J. Corbin and Matthew R. Johnson*

Energy & Emissions Research Lab, Mechanical and Aerospace Engineering, Carleton University, 1125 Colonel By Drive, Ottawa, Ontario K1S 5B6, Canada

S Supporting Information

ABSTRACT: Two complementary analytical methods for quantifying carbon conversion efficiency and species emission rates of gas flares in the form of turbulent nonpremixed flames are derived and tested experimentally. Full mathematical expressions for partial derivative terms necessary to facilitate quantitative uncertainty analysis are also derived and presented as Supporting Information. Key assumptions are individually tested and the resulting generalized expressions are quantitatively compared with several other simplified expressions for calculating flare efficiency found in the literature. The first approach uses a carbon-balance approach to link measured concentrations of diluted combustion products to known flare gas outlet conditions while considering both the dilution of the combustion products and ambient levels of relevant species in the dilution and combustion air. This method is further extended to allow explicit consideration of solid-phase black carbon (soot) that may be present in the products. A second distinct method utilizes a tracer gas injected into the diluted plume to enable quantification of species emission rates from the combustion process directly. Experiments reveal how the two approaches each have advantages in different situations allowing experiments to be better optimized to reduced uncertainties. In addition, the tracer injection method is extensible for use in quantifying efficiencies and liquid-fallout on flares burning a mixed-phase fuel stream.

1. INTRODUCTION

Flaring is the practice of burning unusable or unwanted flammable gas which might otherwise be vented directly to the atmosphere. Ideally, the combustion process would convert 100% of fuel-bound carbon to carbon dioxide. However, under certain conditions (e.g., strong crosswind, low heating value, excess steam- or air-assist) the carbon conversion efficiency can be reduced^{1–6} and the portion of unburned or partially reacted species leaving the flare can increase. Of particular interest are the potential release of unburned methane¹ and black carbon,^{7–9} both of which are potent short-lived climate forcing agents.¹⁰

This paper develops and critiques analytical methods for calculating carbon conversion efficiencies and species emission rates from unconfined, nonpremixed jet flames using gas and particulate samples collected from the plume. The methods each use a system of species conservation equations considering various plume constituents to determine the overall rate of conversion of fuel-bound carbon to carbon dioxide. The robustness of the methods was analyzed using prescribed synthetic test data to mimic the combustion process over a range of anticipated potential conditions and subsequently tested in lab-scale experiments. A quantitative uncertainty analysis was also performed for the various test conditions, and the appropriateness of each method for use in further lab and field experiments is discussed.

2. THEORY

Combustion efficiency, η , can be defined in different ways, however, for the current analysis it will be defined as carbon

conversion efficiency which compares the mass of fully oxidized carbon (i.e., mass of carbon within carbon dioxide) produced by combustion to the mass of carbon in the form of hydrocarbons in the fuel stream:¹¹

$$\eta[\%] = \frac{\text{mass of carbon in produced CO}_2}{\text{mass of carbon in hydrocarbon fuel stream}} \times 100 \quad (1)$$

It is noted that, for cases where $\eta < 100\%$, this definition does not impose any restrictions on the composition or phase of incomplete combustion products. In general these products may include gas phase species such as carbon monoxide and unburned or reformed hydrocarbons, as well as particulate phase soot. In some situations, it may also be useful to define a destruction removal efficiency of any combustible species i in the fuel stream (DRE_i) as

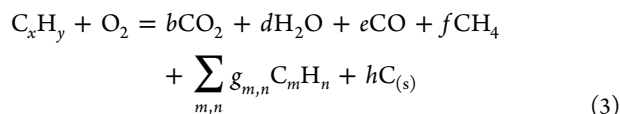
$$\text{DRE}_i[\%] = \left(1 - \frac{\text{production rate of species } i}{\text{flow rate of species } i \text{ in the fuel stream}} \right) \times 100 \quad (2)$$

2.1. General Combustion Efficiency and Species Conservation Equations. Incomplete combustion of a general hydrocarbon fuel or fuel blend (C_xH_y) can be summarized with the following global combustion equation:

Received: July 21, 2014

Revised: October 14, 2014

Accepted: November 5, 2014



The potential products of incomplete combustion may take the form of carbon monoxide (CO), unburned methane (CH₄), unburned and/or reformed gas-phase non-CH₄ hydrocarbons (C_mH_n), and carbon in the form of soot (C_(s)). It is noted that the form of any unburned hydrocarbon species is not restricted to the same form as the hydrocarbons entering in the fuel stream (C_xH_y) or entrained in the ambient air. The summation term, $\sum_{m,n} g_{m,n} C_mH_n$, is thus used to represent all produced non-CH₄ hydrocarbons. The utility of separating CH₄ and C_(s) from C_mH_n in eq 3 will become apparent further in the development where C_(s) may be neglected for the purpose of considering gas-phase-only species, and where the influence of ambient concentrations of CH₄ may be directly considered while ambient concentrations of other species are deemed negligible.

Figure 1 shows a schematic of an arbitrary control volume (CV, represented by the dashed blue line) enclosing the flame,

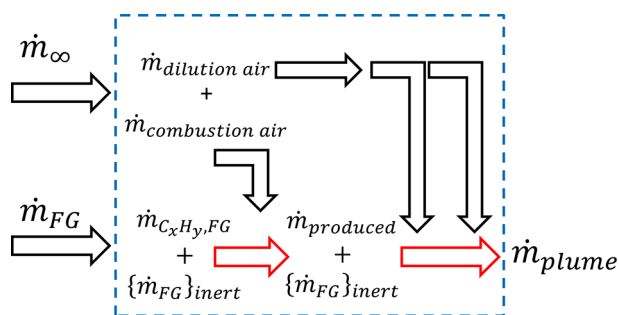


Figure 1. Control volume (CV, indicated by dashed blue line) for combustion process illustrating the overall mass balance defined by eq 3 (sum of terms outside CV) and the breakdown of terms relevant to the species mass balance defined by eq 4.

within which all chemical reactions and product dilution occur. The figure introduces various mass flow rates (\dot{m}) that are important to consider for use throughout the manuscript. Flare gas (\dot{m}_{FG}), and an unknown flow rate of ambient air (\dot{m}_{∞}), enter the CV. Inside the CV, the flare gas is split into hydrocarbons ($\dot{m}_{C_xH_y,FG}$) and diluents ($\{\dot{m}_{FG}\}_{inert}$) that may be present. The ambient air is split into air involved directly in the combustion process ($\dot{m}_{combustion\ air}$) and air entrained during subsequent dilution of the combustion products ($\dot{m}_{dilution\ air}$). The two constituents of the flare gas stream combine with the combustion air and react to release a variety of combustion products ($\dot{m}_{produced}$) as well as any inert species originating in the flare gas. The products are then diluted by the remainder of the ambient air entering the control volume before exiting as the overall plume flow rate (\dot{m}_{plume}).

By considering the CV shown in Figure 1, an expression for the overall mass balance can be derived as follows:

$$\dot{m}_{plume} = \dot{m}_{FG} + \dot{m}_{\infty} \quad (4)$$

Although the present equations are derived with the intent of evaluating combustion from nonpremixed turbulent diffusion flames such as gas flares, the application of the CV illustrated in Figure 1 and the overall mass balance defined by eq 4 are not necessarily restricted to nonpremixed combustion. Since the

choice of CV does not specify whether the mixing of fuel and oxidizer occur across a flame front, as in a nonpremixed configuration, or upstream of the flame, as in a premixed flame, the developed equations may thus be extended to any general hydrocarbon/oxygen combustion system.

Similarly, a species mass balance can be developed for individual species relevant to the combustion process. The mass emission rate of a species i as a component of the diluted combustion products can be written as $Y_{i,plume}\dot{m}_{plume}$, where Y is mass fraction and $Y_{i,plume}$ represents the mass fraction of species i in the diluted plume. The specific species emission rate will depend on the chemical production rate (positive or negative) of species i , $\dot{m}_{i,produced}$; the potential emissions of species i as an inert component of the fuel (i.e., as would occur in a fuel stream containing CO₂ diluent), $\{Y_{i,FG}\dot{m}_{FG}\}_{inert}$, and the rate at which species i is entrained into the plume as an ambient constituent of the entrained air, $Y_{i,\infty}\dot{m}_{\infty}$.

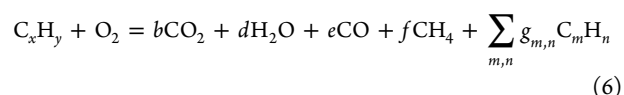
$$Y_{i,plume}\dot{m}_{plume} = \dot{m}_{i,produced} + \{Y_{i,FG}\dot{m}_{FG}\}_{inert} + Y_{i,\infty}\dot{m}_{\infty} \quad (5)$$

Equation 5 implicitly assumes that any trace species (e.g., hydrocarbons or CO₂) present in the combustion air as a constituent of \dot{m}_{∞} do not react. Any potential contribution to the species mass balance due to reactions of these trace species in the combustion air would be negligible relative to the mass of these same species present in air entrained into the plume.¹² Equation 5 further assumes that the constituents of the plume are well mixed such that the composition may be described using a single mass fraction for each species. This well-mixed state is readily achieved in the present experiments where the entire plume is captured and mixed in a duct prior to sampling, and the implications for other sampling systems are further discussed in section 2.2 below.

2.2. Combustion Efficiency and Species Emission Rates Assuming Gas Phase Only Combustion Products.

The initial base case for analysis considers gas-phase products of combustion only, and inherently assumes that any non-gaseous species have negligible contribution to the overall carbon mass balance. This scenario is relevant to flares burning primarily “light” methane-based solution gas, which is a typical flare gas composition in the upstream oil and gas industry.¹³ Available experimental data for turbulent nonpremixed flames burning light hydrocarbon fuels confirm that the proportion of carbon mass emitted in the form of soot is likely negligible. Furthermore, experiments by Pohl et al.⁶ on propane- and propane/nitrogen-fueled vertical diffusion flames established on 3–12” diameter flare burners suggest that soot accounts for less than 0.5% of the fuel carbon mass for these flames. More recent experiments⁷ on lab-scale flares (1–2” diameter) burning primarily methane mixtures consistent with compositions entering solution gas flares in the Alberta upstream petroleum industry,¹³ suggest that soot will account for no more than 0.1% of the combusted carbon by mass.

By considering only gas phase products of combustion, eq 3 simplifies to



Using the relationship between mole and mass fractions, eq 5 can be more conveniently written in molar form since typical gas analyzers measure volume or mole fraction:

$$X_{i,plume}\dot{n}_{plume} = \dot{n}_{i,produced} + \{X_{i,FG}\dot{n}_{FG}\}_{inert} + X_{i,\infty}\dot{n}_{\infty} \quad (7)$$

where X_i denotes the mole fraction of species i , and \dot{n} denotes molar flow rate. The definition of combustion efficiency, eq 1, can similarly be rewritten in molar form where $X_{C_xH_y,FG}$ is the mole fraction of hydrocarbon C_xH_y in the fuel stream and x is the relevant carbon coefficient:

$$\eta[\%] = \frac{\dot{n}_{CO_2,produced}}{x(X_{C_xH_y,FG})\dot{n}_{FG}} \times 100 \quad (8)$$

Destruction efficiency can also be expressed in molar form where $X_{i,FG}$ is the mole fraction of species i in the fuel stream:

$$DRE[\%] = \left(1 - \frac{\dot{n}_{i,produced}}{X_{i,FG}\dot{n}_{FG}} \right) \times 100 \quad (9)$$

In the current lab-scale experiment, the flare is centered under a large collection hood connected to a variable speed exhaust extraction system. The flow rate of the exhaust plume can be directly controlled to provide the lowest possible dilution for a given fuel flow rate, while still capturing the entire product plume. The sampling point is more than 10 m downstream of the duct entrance, and during commissioning of the facility, sample probes were traversed across the duct to verify that gas species mole fractions and soot volume fractions were consistent across the diameter over the range of test conditions.

More generally, in other laboratory setups or especially in field measurement scenarios, it is likely impossible to capture the entire plume. If only a portion of the plume is captured for sampling (e.g., as would occur if single point samples were drawn from a region of the plume), then eq 5 can still be applied so long as the measured species mole fractions in the captured portion of the plume are assumed to be equal to the mean species mole fractions of the entire plume. Alternatively, the developed equations remain valid for determining local combustion or destruction removal efficiencies at a point in the plume, although it should be noted that the relationship between local and overall efficiencies is not necessarily straightforward if spatial variations in velocity and species concentrations in the plume are significant. While experiments in low-turbulence wind tunnels¹² have shown that the plume of a lab-scale flare may be quite inhomogeneous in the near field of the flame (sampling from 1.17 to 1.38 flame lengths downstream of burner exit), these same data suggest that samples drawn from a central region of the plume are representative of the plume as a whole. This latter approach was used in recent field measurements¹⁴ where a 50.8 cm sample intake was used to capture 15–20% of the product volume at several meters (>2 flame lengths) from the burner exit. The sampling system was designed with the intent of sampling a large volume of plume and forcing mixing before the sample was measured. Although possible inhomogeneity of the plume as a function of sampling location was not investigated,¹⁵ additional review of the results from this study suggest that the relative levels of carbon-based species (ratio of CO to CO₂ for example) in the measured plume were well-correlated and independent of time and dilution.

The gas-phase species mole fractions of relevant species in the diluted plume: X_{CO_2} , X_{CO} , X_{CH_4} , and $X_{C_mH_n}$ are all directly measurable using gas analyzers. The flow rate and composition of flare gas are also directly measurable, meaning x , $X_{C_xH_y,FG}$, $\{X_{i,FG}\}_{inert}$, M_{FG} , and \dot{n}_{FG} are also known. By rearranging eq 7 in terms of the species production rate and combining with eq 4

to eliminate the entrained air term, a carbon balance can be derived in which the only unknown term is the plume flow rate.

$$\begin{aligned} x(X_{C_xH_y,FG})\dot{n}_{FG} &= \sum_i \#_{C,i} \left(X_{i,plume} - X_{i,\infty} \frac{M_{plume}}{M_\infty} \right) \dot{n}_{plume} \\ &+ \sum_i \#_{C,i} \left(X_{i,\infty} \frac{M_{FG}}{M_\infty} \dot{n}_{FG} \right) \\ &- \{X_{CO_2,FG}\dot{n}_{FG}\}_{inert} \end{aligned} \quad (10)$$

where $\#_{C,i}$ indicates the number of carbons per molecule of each species in the plume (ie. $\#_{C,i} = 1$ for CO₂ and $\#_{C,i} = m$ for C_mH_n) and CO₂ is assumed to be the only potential carbon-based inert species in the flare gas.

Equation 10 explicitly considers species mole fractions measured in the plume, the exact dilution of the products of combustion, and the contribution by ambient species in the entrained air to the determination of combustion efficiency.

However, the overall mass balance brings in the molecular mass of the plume, M_{plume} , which is unknown and depends on the dilution ratio (where dilution ratio is defined as the volume of air diluting the combustion products over the volume of combustion products) and specific chemical composition of the products. If gas analyzers are capable of measuring water vapor in the plume, M_{plume} can be directly calculated based on the measured volume fraction of CO₂, CO, CH₄, C_mH_n, and H₂O with the assumption that the ratio of N₂ to O₂ in the atmosphere is fixed. Alternatively, it is simpler and ultimately accurate to assume that the molecular mass of the plume is equivalent to that of the ambient air. Even at a low dilution ratio of 10 (which would be difficult to achieve in a practical experiment), the deviation in calculated molar mass of the plume versus that of air is less than 0.5% for flare efficiencies above 80%. The influence of this assumption is further damped in the calculation of efficiency, such that the resultant absolute bias error in the calculated efficiency is less than 5×10^{-3} at an efficiency of 80% and dilution ratio of 10. The effect of assuming $M_{plume} = M_\infty$ is even less pronounced at higher efficiencies and/or higher dilution ratios. With the assumptions that $M_{plume} = M_\infty$ the plume flow rate can be explicitly solved for as shown below.

$$\begin{aligned} \dot{n}_{plume,gas} &= \left[x(X_{C_xH_y,FG})\dot{n}_{FG} + X_{CO_2,FG}\dot{n}_{FG} \right. \\ &- (X_{CO_2,\infty} + X_{CO,\infty} + X_{CH_4,\infty} \\ &+ \sum_{m,n} \#_{C,C_mH_n} X_{C_mH_n,\infty}) \frac{M_{FG}}{M_\infty} \dot{n}_{FG} \left. \right] \\ &/ \left[X_{CO_2,plume} - X_{CO_2,\infty} + A \right] \end{aligned} \quad (11)$$

where

$$\begin{aligned} A &= (X_{CO,plume} - X_{CO,\infty} + X_{CH_4,plume} - X_{CH_4,\infty} \\ &+ \sum_{m,n} \#_{C,C_mH_n} (X_{C_mH_n,plume} - X_{C_mH_n,\infty})) \end{aligned}$$

By substituting the plume flow rate into the species balance equation for CO₂, the efficiency defined in eq 8 can be expressed explicitly as

$$\eta[\%] = \left[x(X_{C_xH_y,FG})B - X_{CO_2,FG}A + (X_{CO_2,\infty}D - X_{CO_2,plume}(X_{CO,\infty} + X_{CH_4,\infty} + \sum_i \#_{C,C_mH_n}X_{C_mH_n,\infty})) \frac{M_{FG}}{M_\infty} \right] / \left[x(X_{C_xH_y,FG})(X_{CO_2,plume} - X_{CO_2,\infty} + A) \right] \times 100 \quad (12)$$

where

$$A = (X_{CO,plume} - X_{CO,\infty} + X_{CH_4,plume} - X_{CH_4,\infty} + \sum_{m,n} \#_{C,C_mH_n}(X_{C_mH_n,plume} - X_{C_mH_n,\infty}))$$

$$B = (X_{CO_2,plume} - X_{CO_2,\infty})$$

and

$$D = (X_{CO,plume} + X_{CH_4,plume} + \sum_i \#_{C,C_mH_n}X_{C_mH_n,plume})$$

In eq 12, it can be noted that all rate terms (fuel hydrocarbon flow rate and gross fuel flow rate) have been removed from the equation and only rate independent mole fractions remain. The conversion efficiency is thus a function of the carbon-based species mole fractions in the plume and ambient air as well as the flare gas composition.

With the plume flow rate defined per eq 11, the emission rate of any species, whether carbon-based or not (e.g., nitric oxide), can be determined by rearranging eq 7 as follows.

$$\dot{m}_{i,produced} = M_i \left((X_{i,plume} - X_{i,\infty})\dot{n}_{plume,gas} - \left\{ X_{i,FG} \frac{\dot{m}_{FG}}{M_{FG}} \right\}_{inert} + X_{i,\infty} \frac{\dot{m}_{FG}}{M_\infty} \right) \quad (13)$$

Using eq 13 and the plume flow rate defined by eq 11, the destruction removal efficiency (DRE_{*i*}) of any combustible species *i* present in the flare gas can be defined as

$$DRE_i[\%] = \left(1 - \left[(x(X_{C_xH_y,FG}) + X_{CO_2,FG}) \times (X_{i,plume} - X_{i,\infty}) + (X_{i,\infty}(X_{CO_2,plume} + D) - X_{i,plume}(X_{CO_2,\infty} + E)) \frac{M_{FG}}{M_\infty} \right] / \left[(X_{i,FG})(X_{CO_2,plume} - X_{CO_2,\infty} + A) \right] \right) \times 100 \quad (14)$$

where

$$A = (X_{CO,plume} - X_{CO,\infty} + X_{CH_4,plume} - X_{CH_4,\infty} + \sum_{m,n} \#_{C,C_mH_n}(X_{C_mH_n,plume} - X_{C_mH_n,\infty}))$$

$$D = (X_{CO,plume} + X_{CH_4,plume} + \sum_i \#_{C,C_mH_n}X_{C_mH_n,plume})$$

and

$$E = (X_{CO,\infty} + X_{CH_4,\infty} + \sum_{m,n} \#_{C,C_mH_n}X_{C_mH_n,\infty})$$

In cases where the combustion efficiency is suitably high, it may be sufficiently accurate and simpler to assume 100% combustion efficiency when calculating the plume flow rate. In this case the carbon balance for combustion considers only CO₂ as a product, and eq 11 simplifies to

$$\dot{n}_{plume,100\%} = \frac{x(X_{C_xH_y,FG})\dot{n}_{FG} + X_{CO_2,FG}\dot{n}_{FG} - X_{CO_2,\infty} \frac{M_{FG}}{M_\infty} \dot{n}_{FG}}{(X_{CO_2,plume} - X_{CO_2,\infty})} \quad (15)$$

The assumption of 100% combustion efficiency can then be relaxed, and eq 15 used instead of eq 11 in combination with eq 13 to derive production rates of other species from their change in measured mole fractions in the plume relative to ambient.

Quantification of the uncertainty in the measured plume flow rate defined by eq 11, combustion efficiency defined by eq 12, gaseous species mass emission rate defined by eq 13, and flare gas species destruction removal efficiency eq 14 can be accomplished using expressions developed in the Supporting Information (SI). The uncertainty on combustion efficiency can be calculated following the instructions in section S.1 in the SI with systematic error defined by eq (S.5) in the SI. For plume flow rate, the uncertainty can be evaluated following the instructions in section S.2 in the SI with systematic error defined by eq (S.7) in the SI. The uncertainty of gas-phase species emission rates can be calculated following the instructions in section S.4.1 in the SI for noncarbon-based species, or section S.4.2 in the SI for carbon-based species with systematic error defined by eqs (S.10) or eq (S.13) in the SI respectively. Similarly, the systematic error for the DRE of a noncarbon-based flare gas species is defined by eq (S.12) in the SI and of a carbon-based flare gas species by eq (S.15) in the SI.

2.3. Comparison with Simplified Expressions for Combustion Efficiency Used in Other Works. A number of different expressions for efficiency have been employed by previous researchers, each of which relies on various simplifications to the method outlined above. The simplifications range from neglecting only the ambient species present in the combustion air to neglecting all ambient concentrations completely, and none of these methods is directly applicable to fuel streams which contain CO₂. To the authors' knowledge, no previous studies have attempted a comprehensive uncertainty analysis of the methods employed, with the possible exception of Bourguignon et al.,¹¹ who considered the uniquely specific problem of flare efficiency measurements in a closed-loop windtunnel. This is not necessarily surprising given the inherent difficulty in fully accounting for entrained ambient species in situations where sampling rates, entrainment rates, and combustion efficiency are all unknown. One of the most robust analysis of combustion efficiency found in the literature¹² neglects the presence of ambient species in the combustion air itself and the possibility of CO₂ as a fuel diluent. An oxygen balance is used to estimate a product dilution factor and corrects the contribution of ambient species to plume levels

Table 1. Various Combustion Efficiency Expressions

McDaniel ¹⁶	$\frac{X_{\text{CO}_2, \text{plume}} - X_{\text{CO}_2, \infty}}{X_{\text{CO}_2, \text{plume}} - X_{\text{CO}_2, \infty} + X_{\text{CO}, \text{plume}} - X_{\text{CO}, \infty} + \sum_{m,n} \#_{\text{C}, \text{C}_m \text{H}_n} X_{\text{C}_m \text{H}_n, \text{plume}} - \sum_{m,n} \#_{\text{C}, \text{C}_m \text{H}_n} X_{\text{C}_m \text{H}_n, \infty} + \text{soot}}$
Pohl ⁶	$\frac{(DF + 1)X_{\text{CO}_2, \text{plume}} - (DF)X_{\text{CO}_2, \infty}}{(DF + 1)(X_{\text{CO}_2, \text{plume}} + X_{\text{CO}, \text{plume}} + \sum_{m,n} \#_{\text{C}, \text{C}_m \text{H}_n} X_{\text{C}_m \text{H}_n, \text{plume}} + \text{soot}) - (DF)(X_{\text{CO}_2, \infty} + X_{\text{CO}, \infty} + \sum_{m,n} \#_{\text{C}, \text{C}_m \text{H}_n} X_{\text{C}_m \text{H}_n, \infty})}$ where $DF = \frac{X_{i, \text{plume}} - X_{i, \text{SR}=1, \text{theoretical}}}{X_{i, \infty} - X_{i, \text{plume}}}$
Poudenx ¹²	$\frac{X_{\text{CO}_2, \text{plume}} - (1 - \alpha)X_{\text{CO}_2, \infty}}{X_{\text{CO}_2, \text{plume}} + X_{\text{CO}, \text{plume}} + \sum_{m,n} \#_{\text{C}, \text{C}_m \text{H}_n} X_{\text{C}_m \text{H}_n, \text{plume}} - (1 - \alpha)(X_{\text{CO}_2, \infty} + X_{\text{CO}, \infty} + \sum_{m,n} \#_{\text{C}, \text{C}_m \text{H}_n} X_{\text{C}_m \text{H}_n, \infty})}$ where $\alpha = 1 - \frac{X_{\text{O}_2, \text{plume}}}{X_{\text{O}_2, \infty}}$
Stroscher ¹⁷	$\frac{X_{\text{CO}_2, \text{plume}}}{X_{\text{CO}_2, \text{plume}} + X_{\text{CO}, \text{plume}} + \sum_{m,n} \#_{\text{C}, \text{C}_m \text{H}_n} X_{\text{C}_m \text{H}_n, \text{plume}} + \text{soot}}$
Torres et al. ⁴	$\frac{X_{\text{CO}_2, \text{plume}} - X_{\text{CO}_2, \infty}}{X_{\text{CO}_2, \text{plume}} - X_{\text{CO}_2, \infty} + X_{\text{CO}, \text{plume}} + \sum_{m,n} \#_{\text{C}, \text{C}_m \text{H}_n} X_{\text{C}_m \text{H}_n, \text{plume}}}$

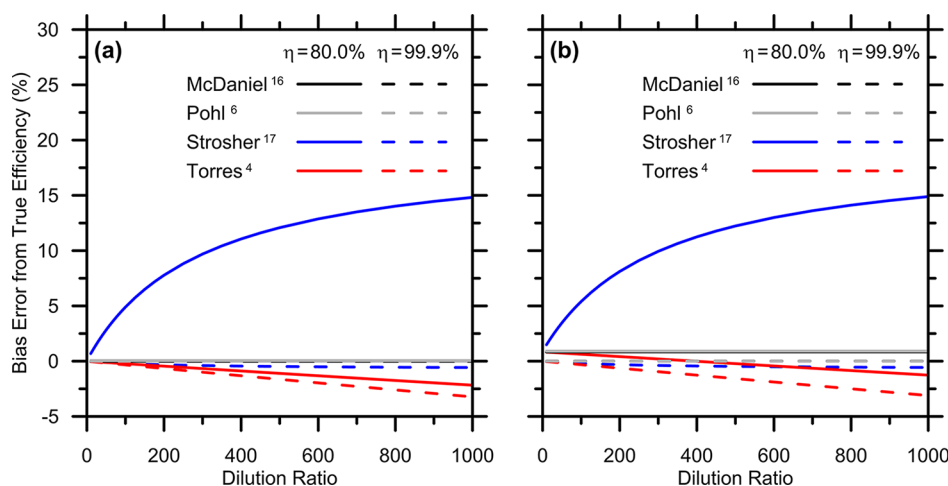


Figure 2. Potential bias errors incurred when using different efficiency expressions (McDaniel,¹⁶ Pohl,⁶ Torres,⁴ and Stroscher¹⁷) as a function of dilution ratio for nominal ambient concentrations of $\text{CO}_2 = 400 \text{ ppm}_v$, $\text{CO} = 1.5 \text{ ppm}_v$, and $\text{CH}_4 = 1.8 \text{ ppm}_v$, where the flare gas contains (a) no CO_2 and (b) 5% CO_2 .

using this factor. Similarly, the method employed by Pohl et al.⁶ corrects for the influence of ambient species concentrations on measured plume dilution by using the theoretical production/consumption of carbon dioxide or oxygen assuming complete combustion to determine a dilution factor. In the mid-1980s EPA flare study,¹⁶ ambient concentrations of all major species were considered by directly subtracting background levels from measured plume values, although the mass balance includes a minor assumption that the volume of combustion air and the ambient species entrained with it are negligible compared to amounts entrained for dilution. In the efficiency calculations shown in the published overview of the recent TCEQ flare study,¹⁴ only ambient CO_2 was considered¹⁴ while other ambient species were neglected. The equation for combustion efficiency for lab-scale and field measurements reported by Stroscher¹⁷ includes no explicit correction for ambient concentrations of carbon-containing species. The combustion efficiency expressions used in the respective studies are summarized in Table 1.

The effect of neglecting or partially neglecting ambient concentrations on the calculated efficiency will vary with both the level of ambient species and the dilution of the products

with entrained air. Each species in the efficiency equations of Table 1 is implicitly or explicitly multiplied by its respective carbon number, $\#_{\text{C},i}$. CO_2 , CO , and CH_4 each has a carbon number of one (one carbon atom per molecule), while $\#_{\text{C},i} > 1$ for higher hydrocarbons. Thus, the effect of neglecting one ambient CO molecule is equivalent to neglecting one CH_4 molecule, with each having half the effect of an ethane (C_2H_6) molecule ($\#_{\text{C},i} = 2$). Figure 2a shows the discrepancy between efficiencies calculated using the equations above and the actual efficiency as a function of dilution ratio assuming nominal ambient concentrations of $\text{CO}_2 = 400 \text{ ppm}_v$, $\text{CO} = 1.5 \text{ ppm}_v$,¹⁸ and $\text{CH}_4 = 1.8 \text{ ppm}_v$.¹⁹ Figure 2b shows the different bias errors incurred if CO_2 is present in the flare gas at 5% by volume. The efficiency expressions defined by McDaniel¹⁶ and Pohl et al.⁶ have distinct bias errors, however the differences are negligible over the conditions shown in Figure 2. Although the maximum dilution ratio in the present experiments is 216, recent airborne field measurements using highly sensitive cavity ringdown gas analyzers²⁰ suggests that dilution ratios of 1000 or more may be relevant in other settings.

For all of the methods, increased ambient levels of any species that are present as products of incomplete combustion

and not corrected for in the equations will result in additional underestimation of the combustion efficiency. Similarly, increased levels of carbon dioxide in the ambient air will result in overestimation of combustion efficiency for methods that do not explicitly include correction for ambient CO₂ levels. If carbon dioxide were present as a fuel diluent, this would induce further bias as it is unaccounted for in the final forms of the equations shown above. Across all dilution ratios and levels of carbon dioxide diluent, the generalized method derived in this paper is able to determine gaseous combustion efficiency within a maximum bias error of less than $5 \times 10^{-3}\%$ (e.g., efficiency [%] of 95 ± 0.005).

2.4. Combustion Efficiency and Species Emission Rates with in Situ Black Carbon Measurement. The calculation approach derived in section 2.2 can be further extended to include direct measurements of emitted carbon mass in the form of soot. Revised species balances as well as a general mass balance are used to produce a carbon balance, which allows for closed forms of plume flow rate, combustion efficiency, and species production rates to be developed. This method includes the same assumptions as the gaseous phase only equations derived in section 2.2, namely nonreacting ambient species, the molar mass of the plume being equivalent to the ambient value, along with the additional assumption that ambient levels of soot in the entrained air can be neglected. The global combustion expression given by eq 3 is utilized, which includes all gas species as well as soot, resulting in mixed-phase products. In the present analysis soot is considered as solid phase molecular carbon, which is consistent with measurements made with laser-induced incandescence (LII).

The species balance equation for soot is

$$\rho_{C(s)} f_{v,plume} \dot{Q}_{plume} = M_{C(s)} \dot{n}_{C(s),produced} \quad (16)$$

where $f_{v,plume}$ is the soot volume fraction in the plume which may be measured using LII or other techniques and $\rho_{C(s)}$ is the density of soot which has an assumed⁹ value of 1860 kg/m³ with an approximate normally distributed standard deviation of 120 kg/m³.

Using the carbon balance technique outlined in a previous section, the plume flow rate can be modified for the inclusion of produced soot:

$$\dot{n}_{plume,gas} = \left[x(X_{C_xH_y,FG})\dot{n}_{FG} + X_{CO_2,FG}\dot{n}_{FG} - (X_{CO_2,\infty} + X_{CO,\infty} + X_{CH_4,\infty} + \sum_i \#_{C,C_mH_n} X_{C_mH_n,\infty}) \frac{M_{FG}}{M_\infty} \dot{n}_{FG} \right] / \left[X_{CO_2,plume} - X_{CO_2,\infty} + \frac{\rho_{C(s)} f_{v,plume} R_u T_{plume}}{M_{C(s)} P_{plume}} + A \right] \quad (17)$$

where

$$A = (X_{CO,plume} - X_{CO,\infty} + X_{CH_4,plume} - X_{CH_4,\infty} + \sum_{m,n} \#_{C,C_mH_n} (X_{C_mH_n,plume} - X_{C_mH_n,\infty}))$$

In eq 17, it is implicitly assumed that the sampled volume of soot particles is negligible relative to the sampled gas volume, such that gaseous species mole fractions obtained using typical gas analyzers which require filtered samples free from particulate are equal to the mole fractions in an unfiltered sample. This is quite reasonable given that measured volume

fractions of soot in the plume are typically of the order of parts per million or less. It is further noted that the use of eq 17 requires measurement of the plume temperature, T_{plume} , and static pressure, P_{plume} , which are necessary to convert the measured soot volume fraction to moles of carbon. Additionally, a correction to the soot volume fraction measured by the LII (or other instrument) must be made to account for differences in temperature between the measurement cell and the plume²¹ as defined below.

$$f_{v,plume} = f_{v,measured} \frac{T_{sample}}{T_{plume}} \quad (18)$$

From eqs 17 and 18, the new closed form equation below can be developed to evaluate combustion efficiency with the inclusion of direct soot measurement.

$$\eta[\%] = \left[x(X_{C_xH_y,FG})B - X_{CO_2,FG}F + (X_{CO_2,\infty}G - X_{CO_2,plume}(X_{CO,\infty} + X_{CH_4,\infty} + \sum_i \#_{C,C_mH_n} X_{C_mH_n,\infty})) \frac{M_{FG}}{M_\infty} \right] / \left[x(X_{C_xH_y,FG})(X_{CO_2,plume} - X_{CO_2,\infty} + F) \right] \times 100 \quad (19)$$

where

$$B = (X_{CO_2,plume} - X_{CO_2,\infty})$$

$$F = (X_{CO,plume} - X_{CO,\infty} + X_{CH_4,plume} - X_{CH_4,\infty} + \sum_{m,n} \#_{C,C_mH_n} (X_{C_mH_n,plume} - X_{C_mH_n,\infty}) + H)$$

$$G = (X_{CO,plume} + X_{CH_4,plume} + \sum_i \#_{C,C_mH_n} X_{C_mH_n,plume} + H)$$

and

$$H = \frac{\rho_{C(s)} f_{v,measured} R_u T_{sample}}{M_{C(s)} P_{plume}}$$

Similar to the scenario in which only gas-phase species are considered, using eq 13 and the plume flow rate defined by eq 17, the destruction removal efficiency (DRE_i) of any combustible species *i* present in the flare gas can be defined as

$$DRE_i[\%] = \left(1 - \left[(x(X_{C_xH_y,FG}) + X_{CO_2,FG}) \times (X_{i,plume} - X_{i,\infty}) + (X_{i,\infty}(X_{CO_2,plume} + G) - X_{i,plume}(X_{CO_2,\infty} + E)) \frac{M_{FG}}{M_\infty} \right] / \left[X_{i,FG}(X_{CO_2,plume} - X_{CO_2,\infty} + F) \right] \right) \times 100 \quad (20)$$

where

$$E = (X_{CO,\infty} + X_{CH_4,\infty} + \sum_{m,n} \#_{C_m H_n} X_{C_m H_n,\infty})$$

$$F = (X_{CO,plume} - X_{CO,\infty} + X_{CH_4,plume} - X_{CH_4,\infty} + \sum_{m,n} \#_{C_m H_n} (X_{C_m H_n,plume} - X_{C_m H_n,\infty}) + H)$$

$$G = (X_{CO,plume} + X_{CH_4,plume} + \sum_i \#_{C_m H_n} X_{C_m H_n,plume} + H)$$

and

$$H = \frac{\rho_{C(s)} f_{v,measured} R_u T_{sample}}{M_{C(s)} P_{plume}}$$

Production rates for a general gas species can be calculated using eq 13 using the plume flow rate term defined by eq 17. Finally, the production rate of soot can be directly calculated as

$$\dot{m}_{C(s),produced} = \rho_{C(s)} f_{v,measured} \frac{R_u T_{sample}}{P_{plume}} \dot{n}_{plume,gas} \quad (21)$$

Quantification of the uncertainty in the measured plume flow rate defined by eq 17, combustion efficiency defined by eq 19, DRE defined by eq 20, and black-carbon emission rate defined by eq 21 can be accomplished using expressions developed in the SI. The uncertainty on combustion efficiency can be calculated following the instructions in section S.1 of the SI with systematic error defined by eq (S.5) in the SI. The uncertainty on the plume flow rate can be calculated following the instructions in section S.2 of the SI with systematic error defined by eq (S.7) in the SI. For black carbon emission rate, the uncertainty can be evaluated following the instructions in section S.4.2 of the SI with the systematic error defined by eq (S.14) in the SI.

2.5. Efficiency Measurements Using a Tracer Injection for Plume Flow Rate Measurement. Although the generalized carbon balance methods outlined in sections 2.2 and 2.3 are suitable for a wide variety of applications, there are cases where an alternate method is desirable, which does not rely on an explicit carbon balance as in eq 10. This would include a situation in which the fuel stream contains a significant liquid fraction that may pass through the flame without burning, and subsequently fall to the ground rather than being entrained with the product plume. Closing the carbon balance via direct measurement of all emitted carbon containing species would not be practically feasible in this situation. However, a substitute equation to use with the system of mass balance equations can be derived following an injection of a nonreacting, measurable gas tracer species into the sampling system that is otherwise not present at appreciable concentrations in ambient air or the products of combustion. Depending on the available measurement technology, it may also be possible to achieve lower overall uncertainties via a tracer-based approach as demonstrated in section 4.

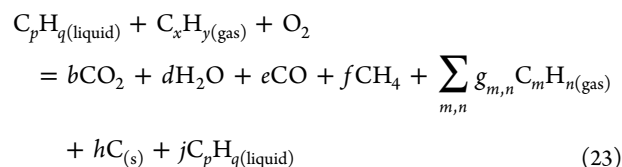
By injecting the gaseous tracer directly into the sampling duct, a simple species mass balance for determining the gas flow rate of the sampled plume can be derived, eq 22, and used to directly quantify the molar flux of captured plume (and hence the molar flux of captured fuel-based carbon).

$$\dot{n}_{plume,gas} = \frac{\dot{m}_{tracer} (1 - X_{tracer}^*)}{M_{tracer} (X_{tracer} - X_{tracer}^*)} \quad (22)$$

In eq 22, X_{tracer} is the measured mole fraction of tracer in the sampling duct while the tracer is being injected, and X_{tracer}^* is the mole fraction of tracer in the plume prior to tracer injection (i.e., when $\dot{m}_{tracer} = 0$). Depending on the choice of tracer species, this background term may be negligible. The uncertainty in the measured plume flow rate, defined by eq 22, can be quantified following the instructions in section S.3 of the SI with systematic error defined by eq (S.8). Corresponding uncertainties in gas-phase species or black-carbon emission rates (defined by eqs 13 and 21), where the plume flow rate is calculated using the tracer-injection method, can be quantified following the instructions in section S.4.1 in the SI with systematic error defined by eqs (S.10) or (S.11) in the SI for gas-phase species and black carbon, respectively. The uncertainties in flare gas species DRE can be quantified following the instructions in section S.4.1 of the SI with systematic error defined by eq (S.12) in the SI.

In an experiment where 100% of the plume-borne carbon is captured (gas and particulate phase), the plume molar flow rate defined in eq 22 can be used in conjunction with eq 13 to calculate species emission rates, which can then be used to determine combustion efficiency via eq 8. Similarly, the destruction removal efficiency for a given flare gas species (eq 2) may be calculated using eq 13 in conjunction with eq 22 to calculate the production rate, and dividing by the flow rate of that species in the flare gas. As shown in the results, this method may lead to reduced uncertainties in calculated species production rates depending on the dilution ratio of the sample and the relative concentrations of species in the plume being measured. Furthermore, as noted above, this tracer-based measurement technique could be utilized with a sampling system capable of capturing 100% of the plume-borne carbon (i.e., gaseous species and soot) to quantify hydrocarbon fallout if liquid constituents were present in the flare stream. In this scenario, the fuel to product mass balance could be closed by directly measuring the plume flow rate via eq 22 and assuming any carbon not captured was in the form of liquid fallout.

The global combustion equation for a mixed phase (gas and liquid) fuelled flare which may emit unburned liquid fuel is



Production rates of all gas species excluding the unburned liquid fuel, $C_p H_q$, can then be defined by eq 24, which is a modified version of eq 13, where subscripts FL and FG indicate liquid and gas phases in the flare stream, respectively. The production rate of soot can be defined by eq 21.

$$\begin{aligned} \dot{n}_{i,produced} = & \left((X_{i,plume} - X_{i,\infty}) \dot{n}_{plume,gas} - \{X_{i,FG} \dot{n}_{FG}\}_{inert} \right. \\ & + X_{i,\infty} \frac{1}{M_{\infty}} (M_{FG} \dot{n}_{FG} + M_{C_p H_q,FL}) \\ & \left. \times \{ \dot{n}_{C_p H_q,FL} \}_{combusted} + M_{tracer} \dot{n}_{tracer} \right) \end{aligned} \quad (24)$$

In eq 24, $\{\dot{n}_{C_p H_q FL}\}_{\text{combusted}}$ is the portion of the liquid fuel that successfully combusts to produce gas phase products and it is assumed that the mean carbon number and molecular weight of the unburned liquid fuel is the same as that of the liquid fuel in the flare stream. From this derivation of species production rates, the liquid fallout can be quantified using the tracer measured plume flow rate eq 22 and a carbon balance of the reaction based on eq 23.

$$\begin{aligned} & \{\dot{n}_{C_p H_q FL}\}_{\text{liquidfallout}} \\ &= \left[x(X_{C_x H_y, FG})\dot{n}_{FG} + p\dot{n}_{C_p H_q FL} + \{X_{CO_2, FG}\dot{n}_{FG}\}_{\text{inert}} \right. \\ & \quad \left. - \sum_i \#_{C_i} K - \frac{\rho_{C(s)} f_{v, \text{measured}} R_u T_{\text{sample}}}{M_{C(s)} P_{\text{plume}}} \dot{n}_{\text{plume, gas}} \right] \\ & \quad / \left[\left(p - \sum_i \#_{C_i} X_{i, \infty} \frac{M_{C_p H_q FL}}{M_{\infty}} \right) \right] \end{aligned} \quad (25)$$

where

$$\begin{aligned} K = & \left[(X_{i, \text{plume}} - X_{i, \infty})\dot{n}_{\text{plume, gas}} + X_{i, \infty} \left(\frac{M_{FG}}{M_{\infty}} \dot{n}_{FG} \right. \right. \\ & \left. \left. + \frac{M_{C_p H_q FL}}{M_{\infty}} \dot{n}_{C_p H_q FL} + \frac{M_{\text{tracer}}}{M_{\infty}} \dot{n}_{\text{tracer}} \right) \right] \end{aligned}$$

3. QUANTIFYING ANTICIPATED UNCERTAINTIES FOR A RANGE OF OPERATING CONDITIONS

The effects of key assumptions were evaluated using synthetic data for which a flare gas composition by volume of 88.01% methane, 7.28% ethane, 3.21% propane, and 1.50% butane was assumed. To estimate the achievable uncertainties associated with each method, a range of flare efficiency and dilution scenarios were simulated using typical bias errors for each input variable. To reduce the number of parameters needed to define the product composition of the synthetic data, the form of the emitted product species was fixed as follows: fuel-bound carbon not fully oxidized to CO₂ was emitted as soot (fixed at 0.1% of the fuel-bound carbon), CO (10% of the non-CO₂ gas-phase carbon), and unburned hydrocarbons (90% of non-CO₂ gas-phase carbon, in the same relative volume fractions as the raw fuel). NO_x emissions were fixed at the EPA suggested emission factor²² of 0.068 lb NO_x / 10⁶ BTU.

For the purpose of calculating uncertainties, the assumed measurement bias uncertainty on gas species concentrations was the larger of 2% of the measured value or a prescribed detection limit for low concentrations (1.0, 0.5, or 0.1 ppm_v depending on scenario), which is typical of many commercial gas analyzers. The concentration of tracer gas in the plume was held at 50 ppm_v independent of combustion efficiency and dilution ratio. The assumed bias uncertainty on measuring the tracer gas was 2 ppb_v, which is attainable with commercially available modern gas analyzers specifically tailored for the chosen tracer species. Soot volume fraction was assumed to be measurable with relative bias uncertainty of 20%, and soot density was assumed to be known to a relative bias of 4% or 75.6 kg/m³ as prescribed by McEwen.²¹ The bias used for the flare gas flow rates in the synthetic cases was 1.25% of the

individual species flow rate, where the total fuel mass flow bias was the root sum of squares of the bias of the individual fuel species. Bias on the plume temperature and pressure was 2.2 K and 15 Pa, respectively.

3.1. Anticipated Uncertainties in Measured Combustion Efficiency. The expected uncertainty on measured combustion efficiency was evaluated considering the products of combustion as defined above. Efficiency was calculated based on each of the three methods derived in sections 2.2, 2.4, and 2.5, and uncertainty was determined using the detailed expressions shown in the SI, which were derived in accordance with ANSI/ASME procedures for estimating uncertainties.²³ The shaded bands in Figure 3a represent the range of possible uncertainty for a given detection limit and dilution ratio over the range of uncertainties tested. The uncertainty in measured efficiency increases as the sample becomes more diluted and the concentrations of various species in the plume approach their respective detection limits. The uncertainties calculated for the gas-phase and mixed-phase expressions were negligibly different for the soot production rate tested (0.1% of fuel-bound carbon), as such only the mixed-phase uncertainties are shown below. Additionally, detection limit changes made a negligible difference on the uncertainty of the tracer injection method as CO₂ concentrations were always high enough so that the uncertainty was dictated by assumed 2% bias on the measured value.

3.2. Anticipated Uncertainties in Measured Species Emission Rates. The calculation of a species emission rate or species yield (mass production rate normalized by fuel mass flow rate) is dependent on the intermediate calculation of the plume flow rate. Two methods are presented for evaluating the plume flow rate based on either an indirect method utilizing a carbon balance as developed in section 2.2, or using a gaseous tracer injection for direct measurement as developed in section 2.5. The inherent advantage of direct plume measurement is that an instrument with high accuracy specifically targeted to measure the chosen tracer gas will result in a uniform uncertainty across all dilution ratios (for a constant tracer concentration), whereas the uncertainty of the indirect method will increase with dilution ratio. Figure 3b plots the relative uncertainties on a general species yield for the two methods at various dilution ratios and species yields. At low yields, the uncertainty grows exponentially as the concentration measured in the plume approaches the detection limit. Product dilution, as mentioned previously, has an important effect on the uncertainty of the indirect method across the range of species yields. For the direct method, product dilution has little effect at high yields until eventually the uncertainties rise as the measured concentrations of the emitted species being quantified approach the detection limit. Thus, at high species yields and/or low dilution ratios, the achievable relative uncertainty for the tracer injection method is approximately 1.35% lower than the carbon-balance method; at low species yields and/or high dilution ratios, the tracer injection method for quantifying species emissions can maintain this improved uncertainty until species detection limits are reached. In the case of 0.1 ppm_v bias error on the species of interest, the difference between the relative uncertainties of the two methods will increase (for a given yield/dilution ratio) making the tracer injection method preferable for quantifying species yields over this range.

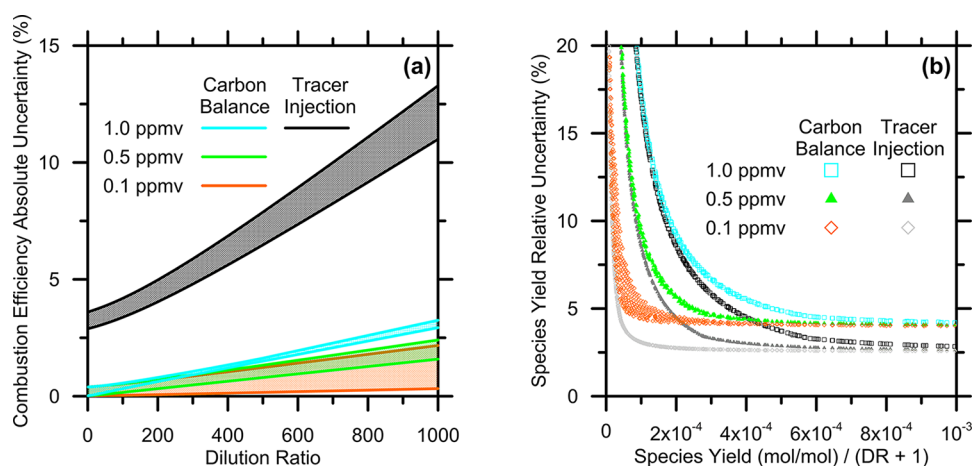


Figure 3. (a) Expected absolute uncertainty on measured combustion efficiency (e.g., $99\% \pm 4\%$ equates to a range of 95–103% at a dilution ratio of 200 using the tracer injection method) evaluated with eq 12 and corresponding SI. (b) Expected relative uncertainty on measured species yield (e.g., 1.0 kg/kg $\pm 10\%$ (0.1 kg/kg)) evaluated using eq 13 with plume flow rate defined by eq 11 (carbon-balance) and eq 22 (tracer injection).

4. DEMONSTRATION EXPERIMENTS AND COMPARISON OF METHODOLOGIES AND UNCERTAINTIES

Measurements utilizing the methods outlined above were taken in April 2014 at the Carleton University lab-scale flare facility. The facility features a modular burner centered under a large hexagonal exhaust hood (3.4 m included diameter), for which the entrance plane is 3.14 m above the floor beneath the burner. The exhaust hood connects to a 40.6 cm round steel duct which provides exhaust extraction using a variable speed fan capable of drawing $\sim 100\,000$ LPM. Sampling is conducted 10.6 m downstream through ports installed in the duct. Samples are drawn through heated sample lines to measurement instruments via vacuum pumps. The flare is operated such that all products of combustion are collected and diluted, which results in a minimum fixed operational exhaust fan setting for a given fuel mass flow rate. As such the dilution of the products is not directly controlled. Gas-phase analysis is accomplished using a MKS 2030 FTIR instrument which measures up to 20 species of interest simultaneously. Reported bias uncertainties for species of interest measured using the FTIR instrument are 0.15 ppm_v, 0.10 ppm_v, 0.15 ppm_v, 0.30 ppm_v, 0.50 ppm_v, and 0.05 ppm_v for CO, CH₄, C₂H₆, C₃H₈, NO, and NO₂, respectively. The tracer gas used in the tests presented was acetylene, and measurement of the tracer gas was conducted with the same gas analyzer previously mentioned. As such, bias uncertainties on the measured tracer concentration was the greater of 2% or 0.3 ppm_v. Soot volume fraction was continuously measured using an Artium LII 200 instrument, with an estimated bias uncertainty of 20%. Four flare gas mass flow rates ranging from 0.488 to 2.15 g/s were tested on a 38.1 mm-diameter flare tip. The fuel was set to consist of 85.24% methane, 7.06% ethane, 3.11% propane, 1.44% butane, 1.91% carbon dioxide, and 1.24% nitrogen, which is consistent with gas flared at battery sites in the upstream energy industry.¹³ Mass flow controllers were individually calibrated to have bias uncertainties averaging $\sim 1.33\%$ of the set point. The relevant data to be examined in this paper are the uncertainties in measured combustion efficiency, soot yield, and various gas species emission rates. Each flare gas flow rate was tested at the maximum fan speed and exhaust flow rate to produce the highest possible dilution for the tested flaring rates. The numbered

Table 2. Experimental Operating Conditions

test number	flare gas flow rate (g/s)	dilution ratio
1	0.488	216
2	0.878	110
3	1.464	65
4	2.147	40

designations for each test, as well as the flare gas flow rate and dilution ratio are outlined in Table 2.

4.1. Combustion Efficiency Measurements and Discussion. Combustion efficiency has been evaluated using the mixed-phase carbon-balance method (section 2.4) and the tracer injection method (section 2.5). The uncertainties on the experimental results as seen in Figure 4a reflect the magnitudes suggested by the synthetic data in Figure 3a. The high precision of the carbon-balance method results from only trace emissions of non-CO₂ carbon-based species relative to the produced CO₂. The much greater uncertainties of the tracer injection method result from the uncertainty on the measured concentrations of carbon dioxide and tracer gas in the diluted plume.

4.2. Calculated Species Yields for Various Methods. Species yields and the associated uncertainties have been evaluated for soot and NO_x as plotted in Figure 4b. The species yields calculated with the carbon-balance and tracer injection methods agree to within $\sim 5\%$ for a given test case and species. This discrepancy is insignificant compared to the uncertainties on the calculated yields. The relative uncertainty for a given test and species is slightly smaller for the tracer injection method when compared to the carbon-balance method, although the difference is limited by the ability to accurately measure the tracer gas with current instrumentation. The uncertainty in soot yield with either method is dominated by the 20% assumed bias on the measured soot volume fraction. For NO_x, the uncertainty is dominated by low plume concentrations relative to the species detection limit. The decreasing relative uncertainties from tests 1 to 4 are a result of decreasing dilution and therefore higher plume concentrations of relevant species. Combustion product dilution ranged from ~ 216 for test 1 to ~ 40 for test 4. In the current experiment, all gas species including the tracer gas were measured using the same instrument (MKS 2030 FTIR Gas Analyzer). Future experiments may allow for the use of a device tailored specifically for

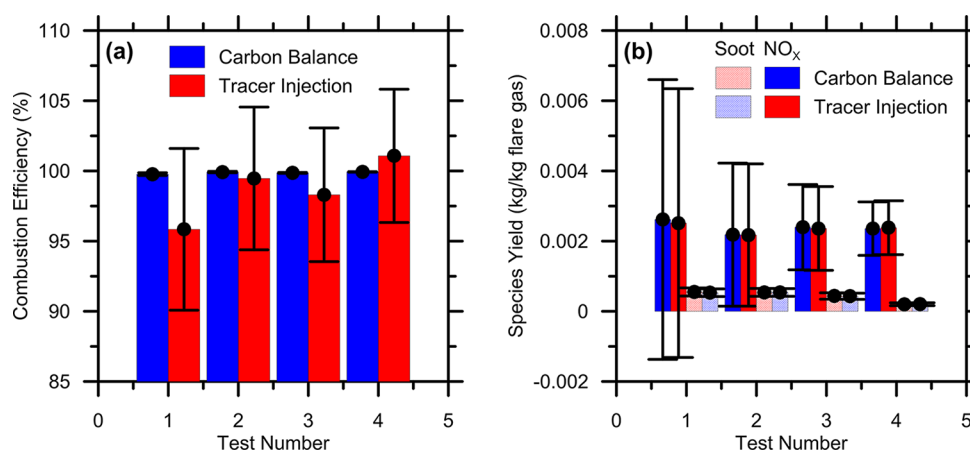


Figure 4. (a) Combustion efficiency and uncertainties calculated using derived carbon-balance and tracer injection methods on a 1.5 in. flare over a range of flare gas flow rates. (b) NO_x and soot species yields and uncertainties calculated using derived carbon-balance and tracer injection methods on a 1.5 in. flare over a range of flare gas flow rates.

measurement of the chosen tracer gas (e.g., cavity ring-down gas analyzers are readily available for the tracer (acetylene) used in the current experiment), which will result in reduced uncertainties for the tracer injection method.

5. CONCLUSIONS

Two complementary analytical approaches were developed for quantifying the combustion efficiency and species emission rates from gas flares represented as turbulent nonpremixed flames. The first approach used a carbon-balance to link known flare gas variables to measurable gas or gas- and particulate-phase (soot) carbon emissions. The second method utilized a tracer gas injected into the diluted combustion plume to enable direct relation of measured species concentrations and emission rates. Detailed expressions were derived to enable quantitative evaluation of measurement uncertainties, and the accuracies of the methods were compared alongside other calculations in the literature over a wide range of potential scenarios. Experiments were also performed to further test and validate the derived methods. Analysis of results revealed that the carbon-balance approach generally provides much lower uncertainties when calculating combustion efficiency. However, for species yields, the experimental data suggest that both methods produce similar uncertainties using the current experimental instruments, and significantly improved uncertainties could be expected when using the tracer injection method with a high-precision analyzer specifically suited for measuring the chosen tracer gas.

■ ASSOCIATED CONTENT

⑤ Supporting Information

Further details of the uncertainty calculations including full mathematical formulations for the sensitivity indices of each input parameter affecting the calculations of combustion efficiency, plume flow rate, and species emission rates for each method. These data will be useful to others wishing to calculate uncertainties in experiments based on the derived methods. Comparisons between predicted uncertainties using synthetic data and measured uncertainties for the present text experiments. This material is available free of charge via the Internet at <http://pubs.acs.org>.

■ AUTHOR INFORMATION

Corresponding Author

*E-mail: Matthew.Johnson@carleton.ca.

Notes

The authors declare no competing financial interest.

■ ACKNOWLEDGMENTS

The authors are grateful for the support of the Canadian Association of Petroleum Producers (CAPP), the Petroleum Technology Alliance of Canada (PTAC), Natural Resources Canada (NRCan) CanmetENERGY Devon, AB, the Texas Commission on Environmental Quality (TCEQ) via Lamar University, and the Natural Sciences and Engineering Research Council of Canada (NSERC).

■ REFERENCES

- (1) Johnson, M. R.; Wilson, D. J.; Kostiuk, L. W. A Fuel Stripping Mechanism for Wake-Stabilized Jet Diffusion Flames in Crossflow. *Combust. Sci. Technol.* **2001**, *169*, 155.
- (2) Johnson, M. R.; Kostiuk, L. W. Efficiencies of Low-Momentum Jet Diffusion Flames in Crosswinds. *Combust. Flame* **2000**, *123*, 189.
- (3) Johnson, M. R.; Kostiuk, L. W. A Parametric Model for the Efficiency of a Flare in Crosswind. *Proc. Combust. Inst.* **2002**, *29*, 1943.
- (4) Torres, V. M.; Herndon, S.; Kodesh, Z.; Allen, D. T. Industrial Flare Performance at Low Flow Conditions. 1. Study Overview. *Ind. Eng. Chem. Res.* **2012**, *51*, 12559.
- (5) Torres, V. M.; Herndon, S.; Allen, D. T. Industrial Flare Performance at Low Flow Conditions. 2. Steam- and Air-Assisted Flares. *Ind. Eng. Chem. Res.* **2012**, *51*, 12569.
- (6) Pohl, J. H.; Lee, J.; Payne, R.; Tichenor, B. A. Combustion Efficiency of Flares. *Combust. Sci. Technol.* **1986**, *50*, 217.
- (7) McEwen, J. D. N.; Johnson, M. R. Black Carbon Particulate Matter Emission Factors for Buoyancy Driven Associated Gas Flares. *J. Air Waste Manage. Assoc.* **2012**, *62*, 307.
- (8) Johnson, M. R.; Devillers, R. W.; Thomson, K. A. Quantitative Field Measurement of Soot Emission from a Large Gas Flare Using Sky-LOSA. *Environ. Sci. Technol.* **2011**, *45*, 345.
- (9) Johnson, M. R.; Devillers, R. W.; Thomson, K. A. A Generalized Sky-LOSA Method to Quantify Soot/Black Carbon Emission Rates in Atmospheric Plumes of Gas Flares. *Aerosol Sci. Technol.* **2013**, *47*, 1017.
- (10) IPCC. *Working Group I Contribution to the IPCC 5th Assessment Report "Climate Change 2013: The Physical Science Basis" - Final Draft Underlying Scientific-Technical Assessment*; Intergovernmental Panel on Climate Change (IPCC): Geneva, Switzerland, 2013; p 2216.

(11) Bourguignon, E.; Johnson, M. R.; Kostiuk, L. W. The Use of a Closed-Loop Wind Tunnel for Measuring the Combustion Efficiency of Flames in a Cross Flow. *Combust. Flame* **1999**, *119*, 319.

(12) Poudenx, P. *Plume Sampling of a Flare in Crosswind: Structure and Combustion Efficiency*. M.Sc. Thesis, University of Alberta: Edmonton, 2000; p. 173.

(13) Johnson, M. R.; Coderre, A. R. Compositions and Greenhouse Gas Emission Factors of Flared and Vented Gas in the Western Canadian Sedimentary Basin. *J. Air Waste Manage. Assoc.* **2012**, *62*, 992.

(14) Allen, D. T.; Torres, V. M. *TCEQ 2010 Flare Study Final Report*; PGA No. 582-8-862-45-FY09-04; Texas Commission on Environmental Quality (TCEQ): Austin, TX, 2011; p 134.

(15) Herndon, S. C.; Nelson, D. D.; Wood, E. C.; Knighton, W. B.; Kolb, C. E.; Kodesh, Z.; Torres, V. M.; Allen, D. T. Application of the Carbon Balance Method to Flare Emissions Characteristics. *Ind. Eng. Chem. Res.* **2012**, *51*, 12577.

(16) McDaniel, M. *Flare Efficiency Study*; EPA-600/2-83-052; United States Environmental Protection Agency: Research Triangle Park, NC, 1983; p 133.

(17) Strosher, M. T. Characterization of Emissions from Diffusion Flare Systems. *J. Air Waste Manage. Assoc.* **2000**, *50*, 1723-1733.

(18) EPA, US; . Carbon Monoxide - National Trends in CO Levels <http://www.epa.gov/airtrends/carbon.html#conat> (accessed Sep 24, 2014).

(19) EPA, US; . Atmospheric Concentrations of Greenhouse Gases http://www.epa.gov/climatechange/pdfs/print_ghg-concentrations-2013.pdf (accessed Sep 24, 2014).

(20) Caulton, D. R.; Shepson, P. B.; Cambaliza, M. O. L.; McCabe, D.; Baum, E.; Stirm, B. H. Methane Destruction Efficiency of Natural Gas Flares Associated with Shale Formation Wells. *Environ. Sci. Technol.* **2014**, *48*, 9548.

(21) McEwen, J. D. N. Soot Emission Factors from Lab-Scale Flares Burning Solution Gas Mixtures. M.A.Sc. Thesis, Carleton University: Ottawa, ON, 2010; p 146.

(22) US EPA AP-42 - *Compilation of Air Pollutant Emission Factors*, 5th ed.; U.S. Environmental Protection Agency (US EPA): Research Triangle Park, NC, 1995; Vol. I, Section 13.5 Industrial Flares; AP-42.

(23) ANSI/ASME. *ANSI/ASME PTC 19.1 - Part 1 - Measurement Uncertainty, Instruments and Apparatus*; New York, NY, United States, 1985.